

Interferometric measurement of refractive index inhomogeneity on polished sapphire substrates: application to LIGO-II

Bob Oreb^{*}, Achim Leistner^{*}, GariLynn Billingsley^{**}, Bill Kells^{**} and Jordan Camp^{**}
CSIRO Telecommunications and Industrial Physics PO Box 218 Lindfield 2070 NSW Australia.

ABSTRACT

In order to improve the detection sensitivity of the Laser Interferometer Gravitational-wave Observatory (LIGO) the use of 40 kg sapphire test masses is being considered for the next instrument upgrade. Currently, sapphire material of adequate size is only available with the optical axis aligned with the m axis of the crystal. To determine the material's suitability it is necessary to characterize the refractive index inhomogeneity of the sapphire substrates for two orthogonal directions of polarisation, to a fraction of a part per million (ppm). We report on a method used to measure the refractive index inhomogeneity which requires three separate measurements of the polished sapphire blank in a Fizeau interferometer. These measurements are of the surface shapes or figures of the two polished sides of the blank and that of the wavefront entering side one propagating through the blank, reflected off side two and exiting through side one. The phase maps corresponding to these three measurements are combined to obtain the refractive index inhomogeneity map distribution.

Measurements were carried out on two sapphire substrates (m axis) produced by the heat exchange method. The inhomogeneity maps show features which depend on polarisation direction. The physical origin of the inhomogeneities is discussed as well as the probable impact on the detection of a gravitational wave signal.

Keywords: Interferometry, gravitational waves, LIGO, metrology, optical inhomogeneity, sapphire.

1. INTRODUCTION

The goal of this effort is to establish the viability of sapphire as a candidate test mass material for the next generation Laser Interferometer Gravitational Wave Observatory¹ (LIGO) detector. The search for astrophysical sources of gravitational radiation will employ long baseline laser interferometers. These include LIGO, the VIRGO project², the TAMA300 project³, and the GEO600 project⁴. All these will employ a variant of a Michelson interferometer illuminated with stabilized laser light. Gravitational radiation will produce a differential length change of the arms of the Michelson interferometer, causing a signal at the output port.

The presence of noise at the interferometer output must be held below the desired strain sensitivity. The primary noise sources defining the interferometer sensitivity are seismic noise at frequencies below 100 Hz, thermal noise between roughly 100 and 300 Hz, and photon counting noise at frequencies greater than 300 Hz. For the initial LIGO detector, the largest contribution to thermal noise comes from the internal motion of the test masses. The amplitude of this motion between 100 and 300 Hz depends inversely on both the mechanical hardness and speed of sound in the chosen test mass material⁵. The test masses in the initial LIGO detector are made from fused silica.

Sapphire is a natural choice to consider as a test mass material for future advanced detectors because its hardness and speed of sound are both larger than those of fused silica, leading to a lower relative internal thermal noise. (Recent investigations have suggested that sapphire's thermal noise may be higher than previously anticipated⁶.) Also, the relatively high thermal conductivity of sapphire may help to lessen problems of thermal distortion due to absorbed laser power. However, a concern in the use of sapphire optics is the presence of bulk optical inhomogeneity due to local distortions of the crystal lattice. The inhomogeneity will cause distortion of the wavefront of the light transmitted through the optic resulting in optical loss.

^{*}Ph: +61-2-94137000, Fax: +61-2- 94137200, email: bob.oreb@tip.csiro.au; ^{**} Caltech , LIGO Project, 51-53 East Bridge Laboratory, Pasadena, California 91125 USA, Ph: 626-395-2129, Fax 626-304-9834, email: Billingsley_G@ligo.caltech.edu.

Sapphire is most commonly grown in the direction of the a- or m-axes. It is a single crystal with trigonal symmetry. The 3-fold axis, also called the optical axis is designated c. The a- and m-axes are perpendicular to c. The rhombohedral cleavage plane, designated r, is inclined at 57.6° from the c-axis in the direction of the m-axis⁷. C-axis material can be cored from a perpendicular growth but the process is not yet in place to provide the 350 millimeter diameter optics which are required for LIGO. The candidate substrates are therefore made from a- or m-axis material. The m-axis material is readily available in large sizes, and so is the first material characterized.

The surface and bulk requirements for LIGO input test masses are extreme⁸. To minimize optical loss the center 120 millimeters of the surface of the test mass must be perfect to within a fraction of a nanometer rms, loss due to bulk inhomogeneity must also be extremely low. The goal of this effort is to establish the viability of sapphire as a candidate test mass material. All measurements reported here are of m-axis material.

Interferometric measurement of refractive index variation in glass blanks has traditionally been carried out by sandwiching a rough ground blank between two polished flats (cover plates) with an index matching oil filling the space between the surfaces. Typically two measurements are made with the configurations shown in figure 1. Firstly the cover plates are brought close together with a thin oil layer separating their polished surfaces. A transmission interferogram is then recorded of the arrangement with the aid of a return flat. For the second measurement the two cover plates are separated and the sample blank inserted between the plates so that the oil (index matching fluid) fills the space between the sample surfaces and the cover plate surfaces. A transmission interferogram is again recorded. The difference of the two recorded interferograms represents the two pass inhomogeneity map of the sample. The advantages of this method are that the blank does not need to be polished or prepared in any special way to measure the homogeneity and it is a relatively quick test. The disadvantages of the method is that it is not very accurate since the index matching is never perfect, the amount of oil in the two configurations is not the same, the oil has different thermal properties to the cover plates and the sample, in one case there is only one layer of oil and two in the other. With this method it is possible to measure the inhomogeneity to an uncertainty of around 0.2ppm.

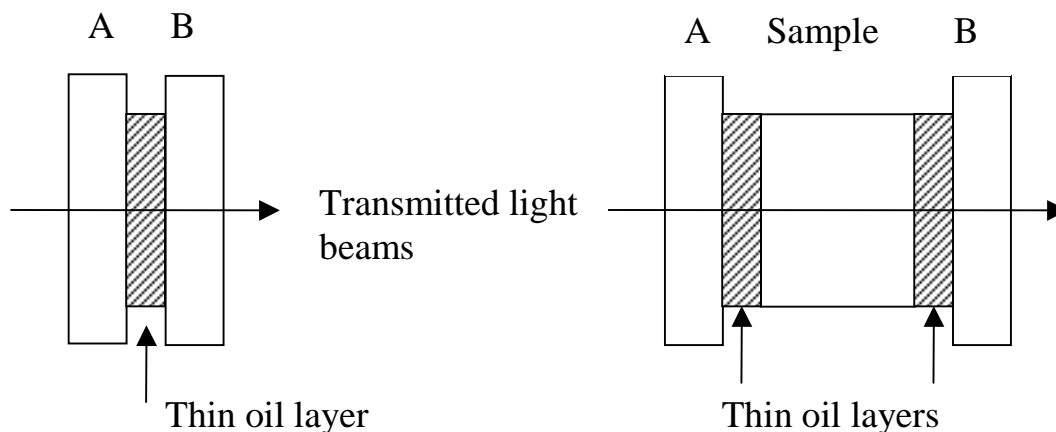


Figure 1: Schematic diagram of the traditional index-matching sandwich method for measuring the refractive index inhomogeneity of a sample

One way to achieve better quality of refractive index inhomogeneity measurement is to polish both sides of the glass blank and carry out direct interferometric measurements on the blank (without the oil or cover plates)⁹ with respect to a reference surface. Here we report on one such method which requires three separate measurements of the polished blank in a Fizeau interferometer.

2. INHOMOGENEITY MEASUREMENTS ON POLISHED SUBSTRATES

Figure 2 shows the three measurement configurations of the test sample in a Fizeau interferometer. These measurements represent the surface shapes or figures of the two polished sides of the blank $S_1(x,y)$ and $S_2(x,y)$ and that of the wavefront entering side one propagating through the blank, reflected off side two and exiting through side one $T(x,y)$.

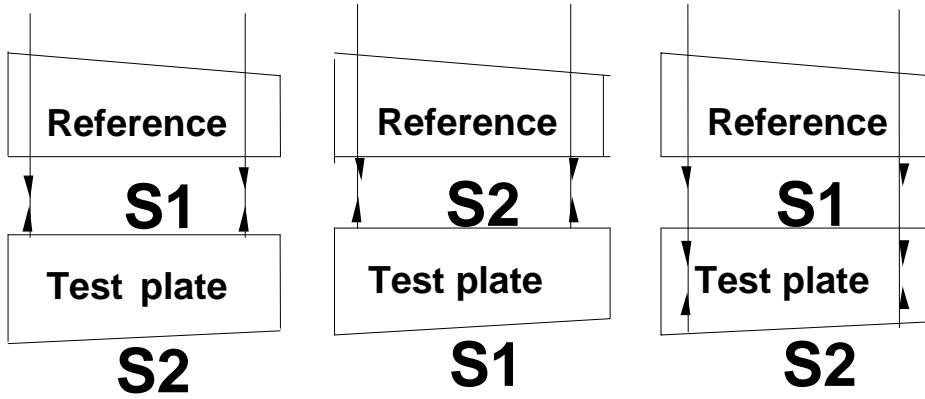


Figure 2: Three measurement configurations

To see how the three measurements need to be combined to give an inhomogeneity map we consider the sample in air (as measured in our interferometer) and trace the paths of the two rays r_1 and r_2 as shown in figure 3.

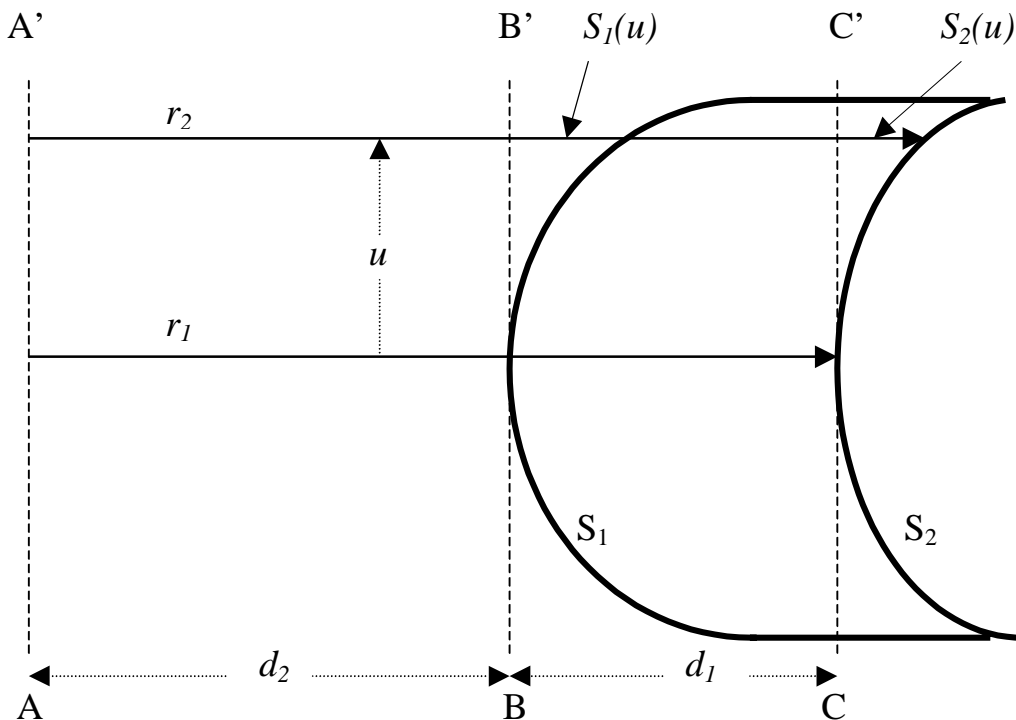


Figure 3: Schematic diagram for ray tracing the optical path through the substrate with respect to a reference plane AA'

Ray r_1 represents the optical path from the reference surface plane (AA') to the back surface (S2) of the substrate, through the center of the substrate. Ray r_2 represents the corresponding optical path at some distance u away from the center of the sample.

If $s_1(u)$ is the distance between surface S1 and the plane BB' (which is tangent to S1 and perpendicular to r_2) along ray r_2 and $s_2(u)$ is the corresponding distance from S2 to the plane CC' along ray r_2 then

$$r_1 = d_2 + d_1 n_0 \quad (1)$$

$$r_2 = d_2 + s_1(u) + [d_1 - s_1(u) + s_2(u)] n(u) \quad (2)$$

where n_0 is the average refractive index of the sample along r_1 , $n(u)$ is the average refractive index of the sample along r_2 , d_1 and d_2 are the perpendicular distances between the various planes as shown in figure 3.

Our Fizeau interferometer measures the optical path represented by $(r_2 - r_1)$. If we let $t(u) = (r_2 - r_1)$, then from (1) and (2)

$$t(u) = s_1(u) - d_1 n_0 + [d_1 - s_1(u) + s_2(u)] [n_0 + \Delta n(u)] \quad (3)$$

where the variation in the refractive index $\Delta n(u)$ is given by

$$n(u) = n_0 + \Delta n(u) \quad (4)$$

Equation (3) can be rewritten as

$$t(u) + s_1(u)(n_0 - 1) - n_0 s_2(u) = [d_1 - s_1(u) + s_2(u)] \Delta n(u) \quad (5)$$

The right hand side of equation (5) represents the inhomogeneity distribution or map as a function of distance u away from the sample's center.

Note from equation (5) if $d_1 \gg s_1(u), s_2(u)$ then

$$\Delta n(u) \cong [t(u) + s_1(u)(n_0 - 1) - s_2(u)n_0] / d_1 \quad (6)$$

2.1 Sign convention

In our interferometer¹⁰ a test wavefront is measured by an area array detector whose pixels are arranged along two perpendicular directions, X and Y. A concave test wavefront is represented as positive optical path or phase while a convex wavefront as a negative phase. By examining the measurement configurations shown in figure 2 it can be seen that the measurement corresponding to equation (3) above is represented by the right hand side configuration of figure 2. It can also be seen, by comparing the middle and the right hand side configurations of figure 2, that the surface S2 is flipped by 180° between the two configurations or setups. Note also that while figure 2 shows only a one dimensional representations of the measurement setup the actual measurements are carried out in two dimensions (i.e. X and Y).

In order to account for the above sign convention, the flipping of the S2 surface (between the middle and the right hand side configurations of figure 2) and to extend the measurements to two dimensions, we make the following transformations:

$$\left. \begin{aligned} s_1(u) &= -S_1(x,y) \\ s_2(u) &= S_2^*(x,y) \\ t(u) &= -T(x,y) \end{aligned} \right\} \quad (7)$$

where $u = \sqrt{(x^2 + y^2)}$,

while $S_1(x,y)$, $S_2(x,y)$ and $T(x,y)$ are the three measurements corresponding to the three configurations of figure 2 and the symbol * designates that $S_2(x,y)$ measurement is flipped by 180° about the Y axis.

With these transformations equation (6) becomes:

$$\Delta n(u) \cong -[T(x, y) + S_1(x,y)(n_0 - 1) + S_2^*(x,y)n_0] / d_1 \quad (8)$$

2.2 Processing the phase maps

Two of the phase maps $S_1(x,y)$ and $S_2(x,y)$ on the right hand side of equation (8) need to be multiplied by a number related to n_0 before they can be added to each other and the map $T(x, y)$. While a special program can be written to do this, an alternative way is to scale the Zernike polynomial coefficients which are fitted to $S_1(x,y)$ and $S_2(x,y)$ phase maps and then regenerate the scaled phase map from the modified coefficients. Our interferogram analysis software¹¹ allows for the phase map to be represented by up to 36 Zernike coefficients. The 36 coefficients for $S_1(x,y)$ and $S_2(x,y)$ were multiplied by a number corresponding to $(n_0 - 1)$ and n_0 respectively and new phase maps generated from these. The two scaled phase maps and $T(x, y)$ are then added on a pixel by pixel basis to obtain the numerator of the right hand side in equation (8). The numerator expression represents the inhomogeneity map.

3. MEASUREMENT RESULTS

3.1 Sapphire substrate

Two polished sapphire substrates (samples A and B) of 150 mm diameter and 80 mm thickness were measured on our phase-shifting Fizeau interferometer operating at a wavelength of 690 nm. The two surfaces of each sapphire substrate were polished to a surface figure which was within ~300 nm of a perfectly flat surface. The sapphire substrates were polished from a boule which was grown in a heat exchange method¹² as an "a-plane" or "m-plane" crystal¹³. As discussed in Section 1, the sapphire crystal suffers from birefringence and inhomogeneity. It was necessary to measure the refractive index inhomogeneity for linearly polarized light in two perpendicular directions ("o" direction which was perpendicular to the crystal's "c" axis and "e" direction which was parallel to it). Two sets of measurements were therefore carried out on each substrate with the polarization direction of the interferometer beam rotated by 90° between the two sets of measurements. Each set of measurements was according to the three configurations of figure 2.

The results for substrate A are shown in figures 4 to 8. Figures 4, 5 and 6 show the three individual measurements according to figure 2 configurations. Figure 7 shows the inhomogeneity map for "o" polarisation derived from these three measurements according to equation (8) and the processing procedure discussed above. This map shows an rms inhomogeneity of 0.36 ppm. Figure 8 shows the corresponding inhomogeneity map for "e" polarisation with an rms inhomogeneity of 0.29 ppm.

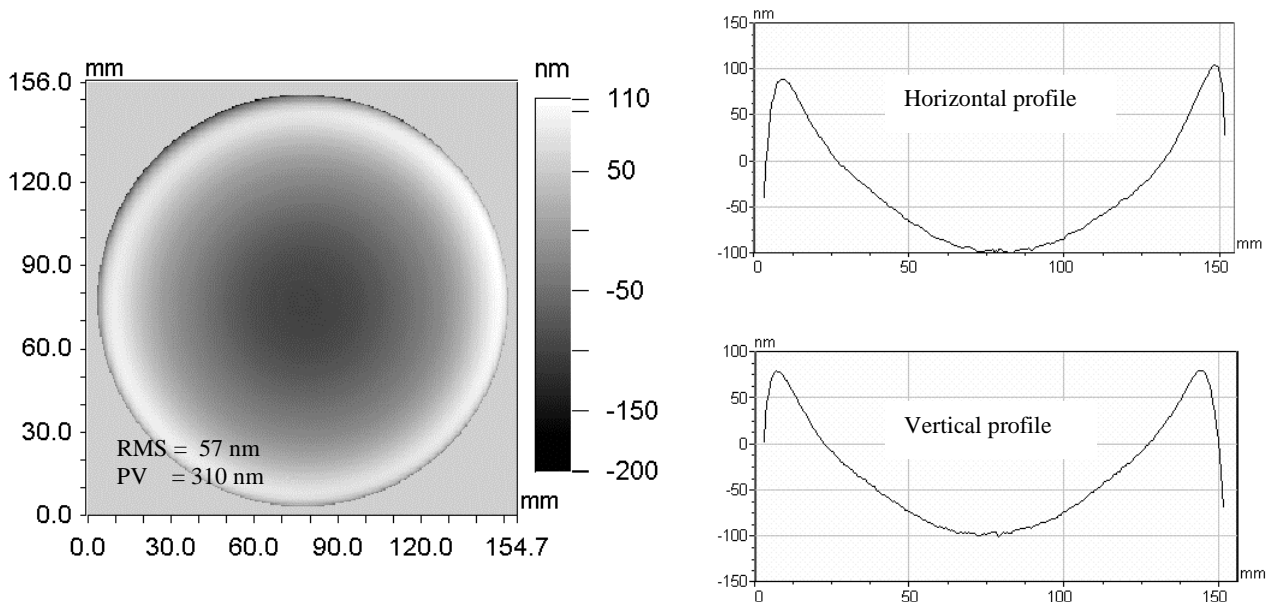


Figure 4: Surface figure phase map of side 1 of substrate A and the two diametral profiles of the map

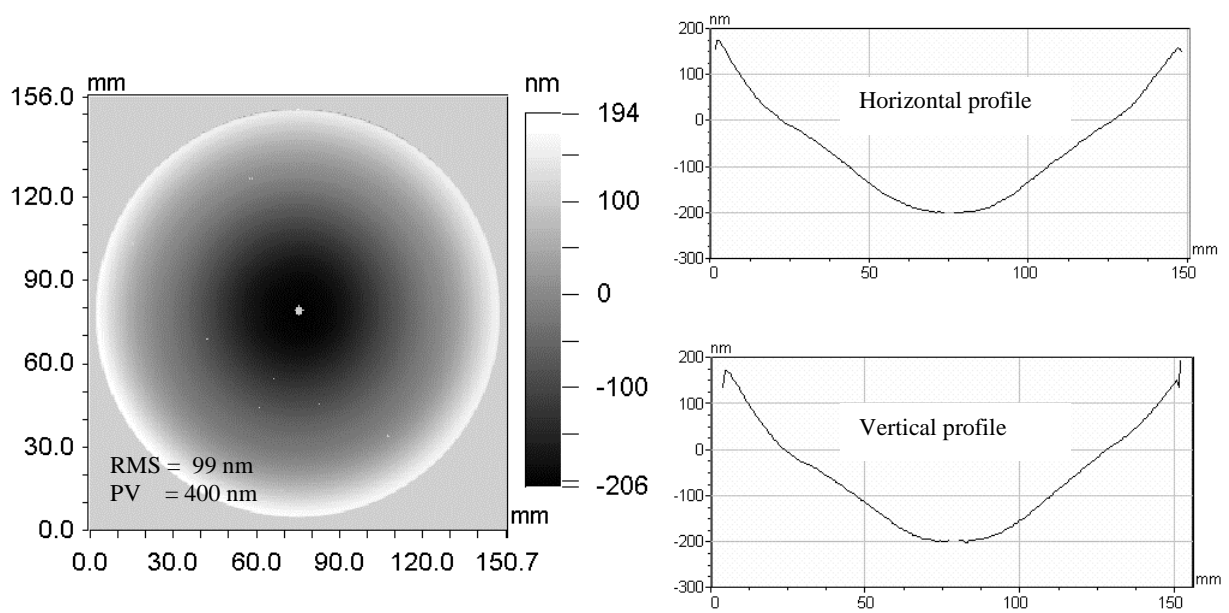


Figure 5: Surface figure phase map of side 2 of substrate A and the two diametral profiles of the map

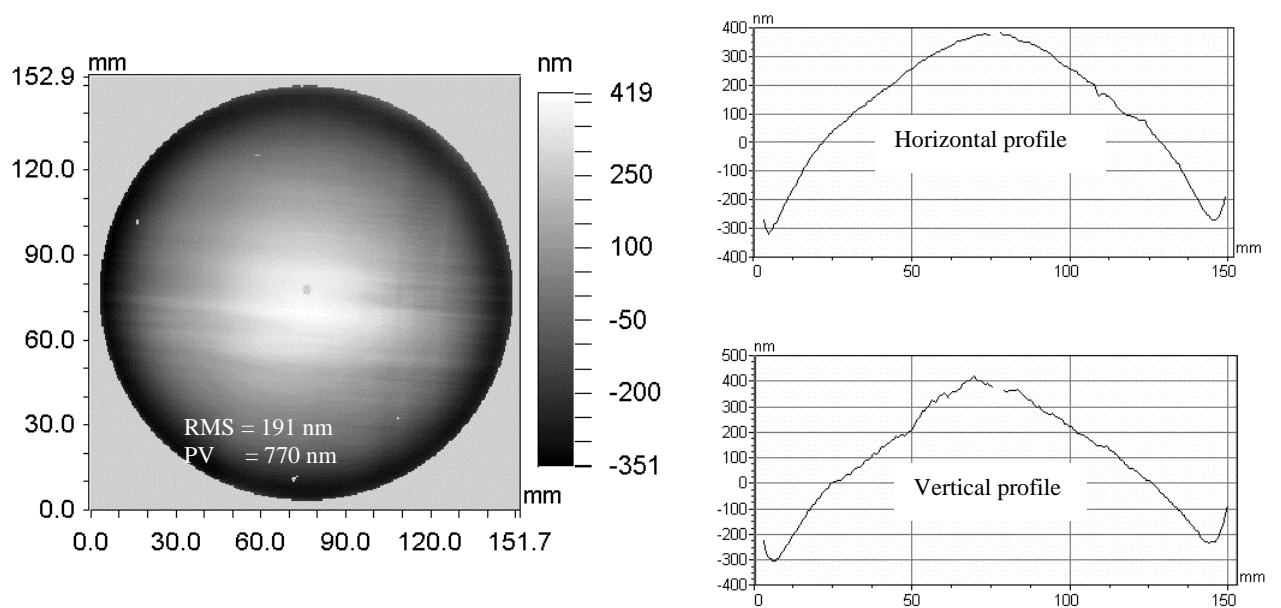


Figure 6: Phase map of transmitted/reflected wavefront of substrate A and the two diametral profiles of the map

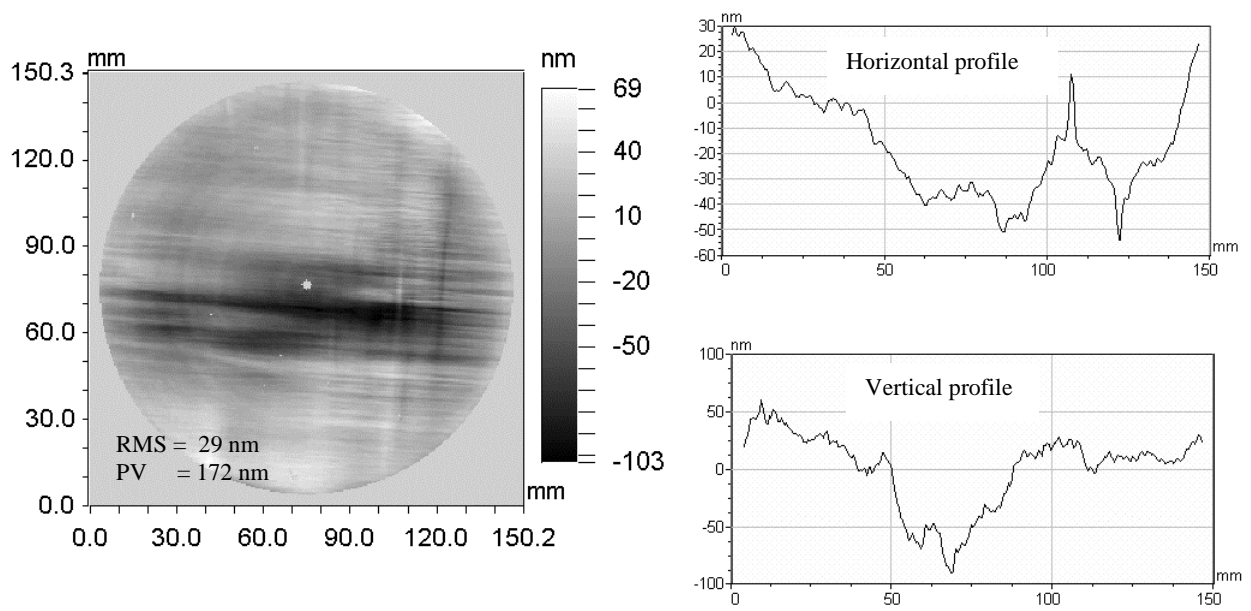


Figure 7: Refractive index inhomogeneity map for the o-polarization of the sapphire substrate A, $\Delta n = 0.36 \text{ ppm}$.

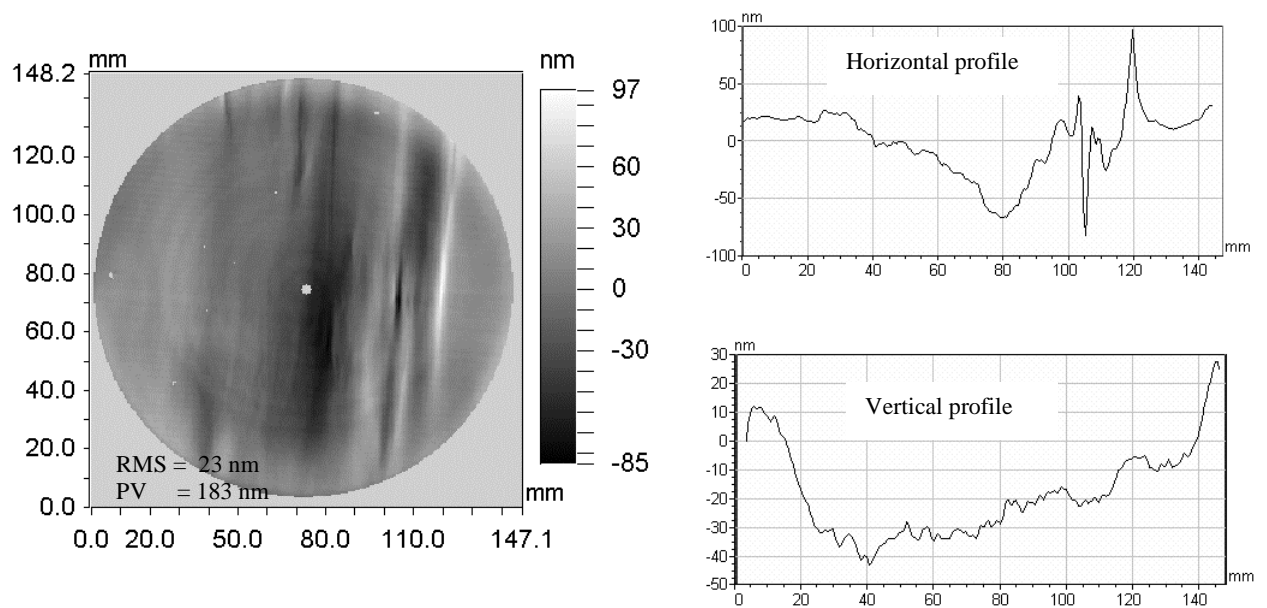


Figure 8: Refractive index inhomogeneity map for the e-polarization of the sapphire substrate A, $\Delta n = 0.29 \text{ ppm}$

Figures 9 and 10 show the refractive index inhomogeneity maps of sample B for the two perpendicular directions (note that the measurements of the individual configurations in figure 2 are not shown for sample B but rather the final calculated inhomogeneity maps derived from equation (8)).

In all the figures 4 to 10 a single pass phase map is shown on the left and two profiles across the phase map on the right. The top profile is located along a horizontal diameter while the bottom profile along a vertical diameter of the phase map. The “o” polarization direction is parallel to the horizontal profile direction and “e” is parallel to the vertical profile direction.

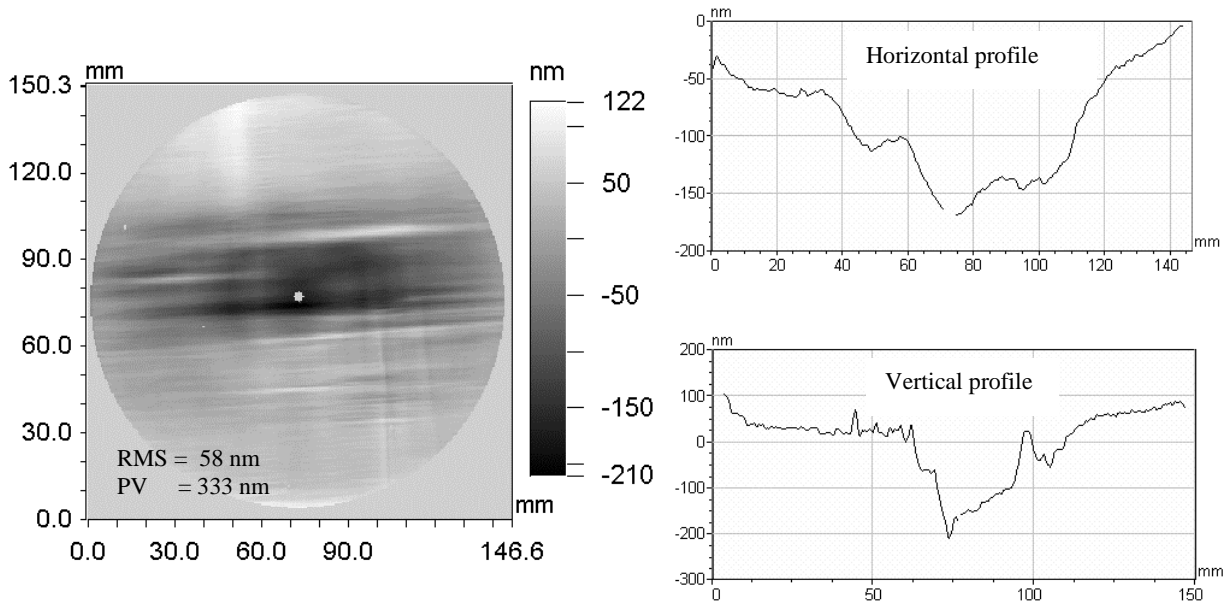


Figure 9: Refractive index inhomogeneity map for the o-polarization of sapphire substrate B, $\Delta n = 0.73 \text{ ppm}$.

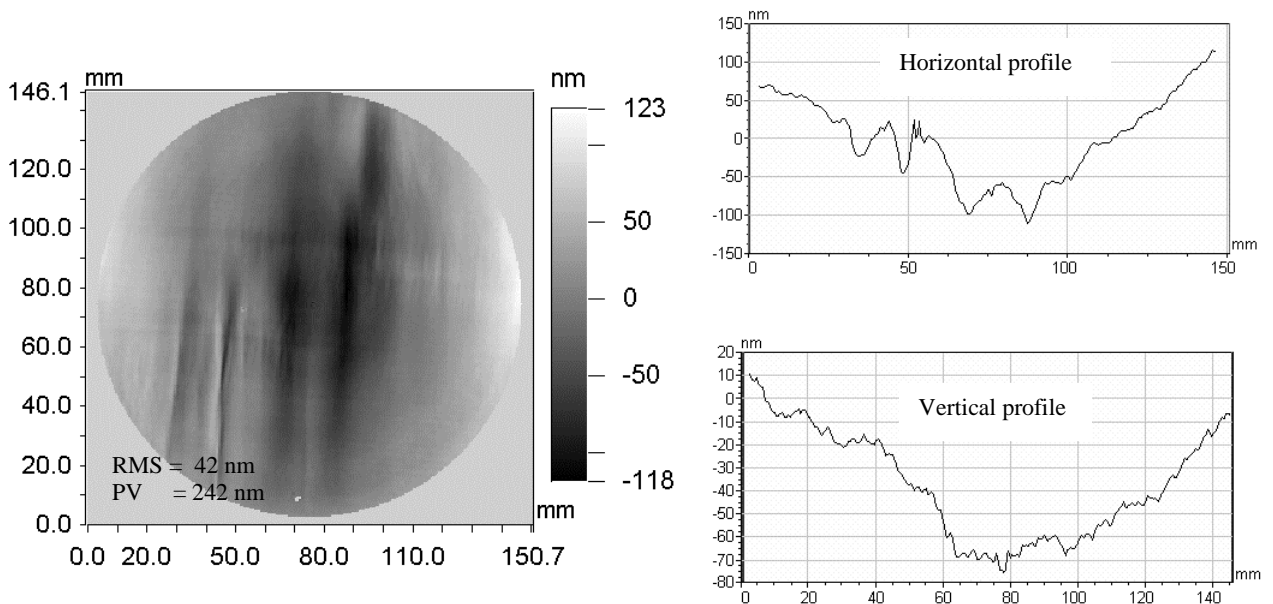


Figure 10: Refractive index inhomogeneity map for the p-polarization of sapphire substrate B, $\Delta n = 0.53 \text{ ppm}$.

3.2 Discussion of inhomogeneity results

It is interesting to note that the appearance, magnitude and orientation of the inhomogeneity depend on the polarisation of the interferometer laser. Features seen strongly in figure 8 can be detected in figure 7, but with much lower magnitude. Of the measurements made thus far, it also appears that the overall magnitude of the inhomogeneity is less when viewed with e polarisation. The most probable, though not only, interpretation of these results is that there is a small, localized wander of the sapphire crystal axis. Using the difference between the index of refraction for the ordinary (o) and extraordinary (e) crystal axes¹⁴ we see that there is an optical path difference of 6×10^{-4} meters over an angle of $\pi/2$ radians. If we assume that the rms path difference of 29 nm (in figure 7) is due to axis wander, then the axes are rotating by $76\mu\text{rad}$ on average.

For LIGO interferometers, OPD distortion of the beam wave front propagating through the central Michelson optics is of concern for the beam splitter and the test mass mirrors ("ITM"s) which couple to the long arm cavities. The critical need for Sapphire substrates pertains to the ITMs, so we mention here consequences of a residual OPD distortion as measured in this study for the ultimate sensitivity of a gravitational wave interferometer. Specifically consider the distortion introduced by identical ITMs having transmission OPD equal to that of the "A" sapphire sample substrate (Figure 7). If the interferometer optics and input laser beam are regarded as otherwise perfect, then it is qualitatively clear that the OPD distortion will scatter some light from the ideal mode determined by the input beam and arm cavity mirrors. The interferometer signal is derived from the parametric modulation of this resonant mode arm cavity field by the passing gravitational wave. Thus any diminution of the arm resonant field, in this instance by the mismatch into the arm by the ITM OPD distortion, will reduce the detection sensitivity directly in proportion. Exactly, the fractional reduction in sensitivity is:

$$(2 \pi (\text{rms OPD}) / \lambda)^2 = 0.03 \quad (9)$$

Here λ is the laser beam wavelength, and the rms OPD is understood to be [Gaussian] weighted according to the beam intensity distribution. The 3 percent value indicated is the appropriate residual extracted from the measurement of sample "A". In terms of interferometer design this degradation is significant, and is only to be regarded as a lower limit since the actual distortions (for instance inevitably different for the two ITMs) will have additional deleterious effects.

Compensating polish is one possible solution to the problem of inhomogeneity in transmissive sapphire optics. This approach has been used in the past to compensate for quadratic homogeneity variation in the first generation LIGO test masses¹⁵. The basis of this technique is removal of material from side two of the transmissive optic, this side is later AR coated so the net result is a compensation of optical path length through the optic. There has not yet been demonstrated compensation for the high spatial frequency features described here. LIGO is pursuing compensating coating and compensating polish in an effort to mitigate the problem of sapphire homogeneity. This will hopefully allow the experiment to benefit from the other highly desirable characteristics of sapphire.

4. CONCLUSION

The hardness, high speed of sound and relatively high thermal conductivity of sapphire make it a desirable candidate for the test mass material to be used in the next generation LIGO detector. The main concern in the use of m-axis sapphire optics is the presence of bulk optical inhomogeneity. The inhomogeneity as reported here will cause distortion of the wavefront transmitted through the optic resulting in an unacceptable loss in detector sensitivity. There are several potential solutions to this problem that are being pursued by the LIGO project. One is ongoing research in growing c-axis sapphire. Another is the full characterization of a-axis sapphire. Third is a research program using compensating polish and coating, to address the high spatial frequency inhomogeneities reported here. Finally, the design fallback for the next generation LIGO detector is to use fused silica for all optics.

The method for measuring the refractive index inhomogeneity described in this paper allows very accurate and detailed characterisation of the material's refractive index variation. This is very important for precision optics used in transmission. The main contribution to the measurement error comes from the third configuration of figure 2 in which the reflected/transmitted wavefront is measured. This configuration is susceptible to thermal gradients in the substrate being measured especially if the material has a long thermal time constant or has a high temperature coefficient of refractive index variation. With sapphire thermal conductivity is quite good and so the thermal gradients across the

substrate settle down relatively quickly (within an hour or so) as long as the measurement environment is stable. An additional potential drawback of this measurement technique is that the substrate needs to be reasonably well polished on both sides.

We acknowledge the assistance of C.J. Walsh, J.A. Seckold, Z.S. Hegedus and N. Savvides. Discussions with Chandra Khattak of Crystal Systems and Roger Route of Stanford University are gratefully acknowledged. This material is based upon work supported by the National Science Foundation under the Co-operative Agreement with the California Institute of Technology, No. PHY-9210038.

5. REFERENCES

1. A. Abramovici, W. Althouse, R.W.P. Drever, Y. Gursel, S. Kawamura, F.J. Raab, D. Shoemaker, L. Sievers, R.E. Spero, R.E. Vogt, R. Weiss, S.E. Whitcomb, M.E. Zucker, "LIGO: The Laser Interferometer Gravitational-Wave Observatory," *Science* **256**, 325-333, 1992.
2. A. Giazotto, "The Virgo Experiment: Status of the Art", in *First Edoardo Amaldi Conference on Gravitational Wave Experiments*, E. Coccia, G. Pizella and F. Ronga (eds.), 86-99, (World Scientific, Singapore, 1995).
3. K. Tsubono, "300-M Laser Interferometer Gravitational Wave Detector (TAMA300) in Japan", in *First Edoardo Amaldi Conference on Gravitational Wave Experiments*, E. Coccia, G. Pizella and F. Ronga (eds.), 112-114, (World Scientific, Singapore, 1995).
4. K. Danzmann, "GEO600 - A 600 m Laser Interferometric Gravitational Wave Antenna", in *First Edoardo Amaldi Conference on Gravitational Wave Experiments*, E. Coccia, G. Pizella and F. Ronga (eds.), 100-111, (World Scientific, Singapore, 1995).
5. A. Gillespie and F. Raab, "Thermally excited vibrations of the mirrors of laser interferometer gravitational-wave detectors", *Phys Rev D* **52**, 577-585, 1995.
6. V. Braginsky, M. Gorodetsky, S. Vyatchanin, "Thermodynamical fluctuations and photo-thermal shot noise in gravitational antennae", *Phys. Lett A* **264**, 1-10, 1999.
7. D. Harris, F. Schmid, D. Black, E. Savrun and H. Bates, "Factors that influence mechanical failure of sapphire at high temperature", *Proc. SPIE, Vol.3060, Conference on Window and Dome Technologies and Materials V*, Orlando, FL, 226-236, 21-22 April 1997.
8. S. Whitcomb, G. Billingsley, J. Carri, A. Golovitsner, D. Jungwirth, W. Kells, H. Yamamoto, B. Bochner, Y. Hefetz, P. Saha, R. Weiss "Optics Development for LIGO", *Proc. of the TAMA international workshop on Gravitational Wave Detection*, November 11-12, 1996, Saitama, Japan, K. Tsubono, M.-K. Fujimoto, and K. Kuroda, eds., Universal Academy Press, Inc., Tokyo, 229-239, 1997.
9. A. Fanning, J. Ellison and D. Green, "Polished homogeneity testing of Corning fused silica boules", *Proc. SPIE Vol. 3782, 44th Annual Conference on Optical Manufacturing and Testing III*, Denver USA, July 1999.
10. P.S. Fairman, B.K. Ward, B.F. Oreb, D.I. Farrant, Y. Gilliland, C.H. Freund, A.J. Leistner, J.A. Seckold and C.J. Walsh, "A 300 mm aperture phase-shifting Fizeau interferometer," *Opt. Eng.* **38**, 1371-1380, 1999.
11. Veeco Vision software, 2650 East Elvira Road, Tucson, Arizona 85706 USA.
12. F. Schmid and D. Viechnicki, "Growth of Sapphire Disks From the Melt by a Gradient Furnace Technique," *J. Am. Ceram. Soc.* **53** (9), 528-529, 1970.
13. C.P. Khattak, F. Schmid and M.B. Smith, "Correlation of Sapphire Quality with Uniformity and Optical Properties," *Proc. SPIE, Vol.3060, Conference on Window and Dome Technologies and Materials V*, Orlando, FL 21-22 April 1997.
14. "Electro-Optics Handbook", pp 11.13-11.23, Ronald Waynant and Marwood Ediger Editors, McGraw-Hill Inc., 1994.
15. C. J. Walsh, A. J. Leistner, B. F. Oreb, J.A. Seckold, D. I. Farrant and E. Pavlovic "Metrology of transmission optics for LIGO," *Proc. SPIE Vol. 3744, Interferometry' 99*, Poland, 18-30, Sept. 1999.